ABSTRACT

Design of an Experimental Arrangement for the Detection of Neutral Fragments Produced in Electron Molecule Collisions.

Dhurba Raj Sapkota, M.S.

Mentor: Wickramasinghe Ariyasinghe, Ph.D.

Existing experimental and theoretical values of the production cross sections of neutral fragments of electron and methane (CH_4) collision have been studied. Possible neutral production cross sections of CH_4 are estimated using the production cross sections of ionic fragments, elastic and total scattering cross sections obtained experimentally by different groups in the electron energy range 100-500eV. The estimated cross sections are in the range of low $10^{-16}cm^2 to$ low $10^{-17}cm^2$. Using the similar approach with existing theoretical cross sections, above estimated range of neutral production cross sections is confirmed. Using these estimations, the time of flight based experimental arrangement is designed and under development to measure the productions cross section of neutral fragments.

Design of an Experimental Arrangement for the Detection
of Neutral Fragments Produced in Electron Molecule Collisions

by

Dhurba Raj Sapkota, B.S.

A Thesis

Approved by the Department of Physics

Gregory A. Benesh, Ph.D., Chairperson

Submitted to the Graduate Faculty of
Baylor University in Partial Fulfillment of the
Requirements for the Degree
of

Master of Science

Approved by the Thesis Committee

Wickram Ariyasinghe, Ph.D., Chairperson

Kenneth T. Park, Ph.D.

Dwight P. Russell, Ph.D.

Ron Morgan, Ph.D.

Accepted by the Graduate School

August 2014

J. Larry Lyon, Ph.D., Dean

Page bearing signatures is kept on file in the Graduate School.

TABLE OF CONTENTS

LIST OF FIGURES

LIST OF TABLES

.

ACKNOWLEDGMENTS

I am extremely grateful to Dr. Ariyasinghe Wickramasinghe for giving me an opportunity to do a master thesis under his supervision. I would like to express my sincere gratitude to him for his useful comments, remarks and involvement through the learning process of this master thesis. Besides my supervisor, I would like to thank my thesis committee members: Dr. Kenneth T. Park, Dr. Dwight P. Russell and Dr. Ronald Morgan for their precious time and encouragement. I also want to thank the faculty members, staff and my fellow students of Department of Physics at Baylor University for their kind support.

Last but not the least, I would like to thank my family and would like to dedicate this work to them.

CHAPTER ONE

Introduction

.

1.1 Neutral Fragments in Electron Molecule Collision

The interaction between fast moving electrons and molecules results in excitation, fragmentation and ionization of molecules. These processes occur mainly by two paths; (1) direct ionization of the molecule by fast moving electrons, and (2) excitation of the molecule by fast moving electrons into any dissociative state of the molecule and reduce it into ionic and neutral fragments. The excitation, fragmentation and ionization of a diatomic molecule (xy) can be summarized [1-2] in following ways

e+ $xy \rightarrow (xy)^{*}$+e excitation (i)

e+ $xy \rightarrow x$+ y+e neutral fragmentation (ii)

e+ $xy \rightarrow xy^{+}$+2e ionization (iii)

e+ $xy \rightarrow x^{+}$+y +2e

$\rightarrow x^{+} + y^{-}$+e dissociative ionization (iv)

The cross sections for excitation and neutral fragments production are much more difficult to measure than those for ionization because of the difficulty involved in detecting the neutral products. Direct detection of neutral fragments is impossible since those don't interact with electric or magnetic fields, like charged particles. If one wishes to detect them, there should be a secondary ionization mechanism for neutrals.

The production cross sections of fragments become important due to their application in industry, including aspects of the atmosphere and space science [3-6].

Etching of semiconductor is a most important technique used in the industry. This is a technique which refers to the removal of material by exposing the material to a bombardment of ions that dislodge portions of the material from the exposed surface. For instance, in the fabrication of optoelectronics devices, dry etching is used mostly. Dry etching involves gas-phase reactions (usually in plasmas) that form highly reactive species which impinge on the surface to react with the surface, to erode the surface, or both.

The common example of the material which is used in the fabrication of optoelectronic devices is Indium Phosphide (InP). Reactive ion etching (RIE) is one technique which is used to etch InP. RIE involves the formation of highly reactive ions, in plasma; these ions are used to erode the surface by bombarding them on the surface. Formation of the ions in plasma takes by the following ways

e +Ar → + e	excitation
e + 2Cl +e	dissociation
e + Ar → + 2e	ionization
e + → +Cl + 2e	dissociative ionization

Sputter is a first technique which is used to erode InP from the surface of a semiconductor. In this technique semiconductor surface is bombarded with high-energy argon ion that knocks InP off the surface without any reaction. The second technique is by a reaction which takes place between InP and chlorine to form InCl. By a series of chemical reaction with Cl and InCl, finally, solid InCl_3 is formed, which goes away from the surface after vaporization or is kicked off the surface by impingement of a high-energy argon atom.

Silane(SiH_4) is another constituent of low-temperature processing plasmas employed in the fabrication of Si-based microelectronic devices and other semi-conducting components. SiH_4 is also a constituent of the atmosphere of the planet Saturn and the minor constituents of the atmospheres of several other planets and satellites[7]. In the industry as well as in the atmosphere, dissociation of SiH_4 by electron collision is very important in understanding of chemical composition at those places.

In astrophysics, production cross section of molecular fragments is in interest for the applications of the atmosphere in Titan, the largest moon of Saturn. Like the atmosphere of Earth Titan's atmosphere near the surface is dominated by molecular nitrogen. Titan orbits Saturn at a distance of 20.6 R_s[Radius of Saturn (R_s) $\sim$ 60268 kilometer], which is inside Saturn's magnetosphere. H^+ , N^+ and O^+ are the major magnetospheric ions near the orbit of Titan [8]. Titan is in direct contact with the solar wind. Titan doesn't appear to have an intrinsic magnetic field, so the ions come to interact with the neutrals in the corona (a type of plasma that surrounds the sun and other celestial bodies). This result can produce heating, collisional ejection of atoms and molecules, and expansion of corona. Therefore, it is important to understand the production of fragments to study the expansion of corona.

Production cross sections of fragments by electron impact process play a major role in Earth's atmosphere. Sun's rays bombard the Earth's atmosphere and there occurs photoionization in the upper part of the Earth's atmosphere. Photoionization in fact is the dissociative ionization which breaks the ionosphere of ammonia, methane, carbon dioxide, and other existing gases to form free atoms of oxygen and nitrogen those results in molecular oxygen and nitrogen.

It is believed that the simple hydrocarbons are the major constituent in the planetary and cometery atmosphere. They play an important role in edging plasmas of magnetically confined high temperature hydrogen plasma [9]. Therefore, simple hydrocarbon molecules have received much interest in the area of electron induced fragmentation as a prototype of polyatomic molecules. As a result, these molecules have been studied in many laboratories as in Ref.10 and the references therein.

The molecule of methane (CH_4) is the simplest compound in the hydrocarbon series. Also, it is the main representative of the organic substances in the Earth's atmosphere. Experimental and theoretical cross sections of ions production are limited in the interaction of low-energy electrons with methane molecules, in particular, the formation of positive ions and neutrals. Upon electron impact, the methane molecule can decompose into various neutral and ionic fragments whose abundances are in the decreasing order from $CH_3, CH_2, CH, C\ and\ H$ for neutrals and

for ions [2,6]. The electron interaction process of CH_4 can be summarized as shown below

e+$CH_4 \rightarrow (CH_4)^*$ +e	excitation
e+$CH_4 \rightarrow CH_3 + H^+ +$ 2e	neutral fragmentation
$\rightarrow CH_2 +$ + 2e	
$\rightarrow CH_2 + H + H^+ +$2e	
$\rightarrow CH + H_2 + H^+ +$2e	
$\rightarrow CH + H_3^+ +$2e	
$\rightarrow C + H_2^+ + 2H +$2e	
$\rightarrow C + H + H_3^+ +$2e	
e+$CH_4 \rightarrow$ +2e	ionization
e+$CH_4 \rightarrow$ $+ H +$ 2e	dissociative ionization
$\rightarrow$ $+H^- +$e	
$\rightarrow$ $+H_2 +$2e	
$\rightarrow CH^+ + H + H_2 +$2e	

$\rightarrow CH^+ + H^- + H_2 + e$
$\rightarrow C^+ + 2H_2 + 2e$
$\rightarrow H^+ + C + 3H + 2e$

Almost all the ions or neutrals are resulted from more than one path (channel). In an experiment one might study the production cross section of a particular item for the whole process but not for a given channel.

1.2 Existing Experimental and Theoretical Data for Neutral Fragments of Electron Methane (CH_4) Collision

There are many experimental and theoretical studies on fragmentation of CH_4 into various ions after interacting with energetic electrons. But, very few experimental attempts are done to detect the neutral fragments because of the difficulties associated with the accurate detection methods, as explained earlier. Also the theoretical work in this area of research is not very abundant. Only three experimental attempts have been found in the literature for detection of neutral fragments in CH_4 and electron collisions. The outcomes of these experimental observations are not in agreement with each other's in overlapping energy ranges.

The first measurement of the production cross section of the neutral fragments CH_3 and CH_2 produced by electron CH_4 collisions was made by Tohru Nakano, Hirotaka Toyoda and Hideo Sugai in 1991[11]. Schematic of their experimental set up is shown in the figure 1.1. This set up is based on two electron beams and Quadrupole mass spectrometer (QMS). There are three chambers which are differentially pumped with two turbo pumps. In the first chamber primary beam of electrons are produced from a biased hot filament. In the second chamber, primary electron beam interacts with methane at a pressure in the range 10^{-7}- 10^{-3} Torr, and the electrons collected by a cylindrical

collector. In the third chamber the electron beam coming from a second filament selectively ionizes neutral radicals effusing from the dissociation cell through orifice into an ionization chamber. The ionized radicals are separated by QMS; the output pulses from a secondary electron multiplier in the QMS system are counted and processed by a computer. The production cross section of neutral fragments CH_3 and CH_2 (in the order of $10^{-16} cm^2$) determined in this experiment are displayed in the figure 1.4 as a function

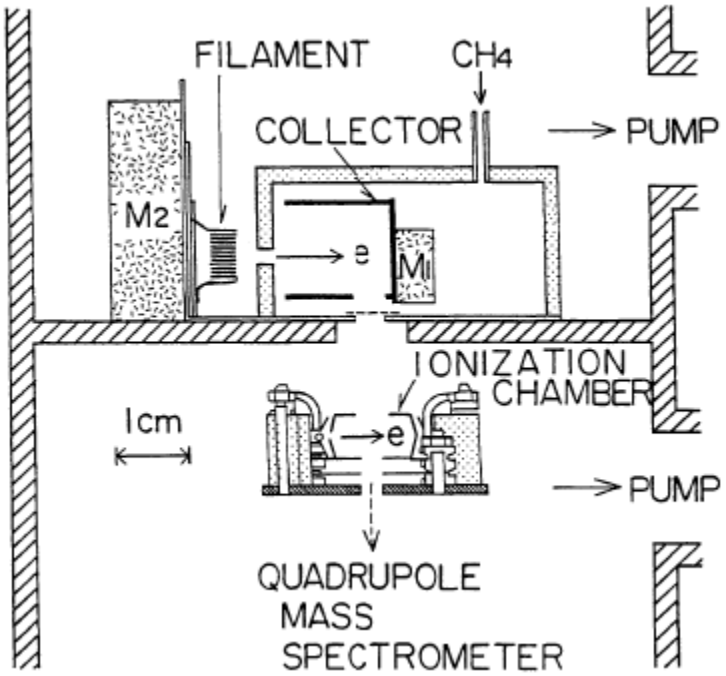

Fig.1.1. Experimental set up for the measurement of neutral fragments and produced by electron CH_4 collisions in Ref. 11.

of bombarding electron energy. In the same figure, the production cross sections of neutral fragments determined by Safa Moltagh and John H.Moore [12] and Makochekanwa et al. [1] are also displayed for comparison. The experimental method reported in Ref.12 and Ref.1 will be introduced next.

In 1998, Safa Moltagh and John H. Moore [12] developed a technique to determine the cross sections for the neutral fragments of methane. The schematic of the apparatus used is as shown in the figure 1.2. It consists of two chambers; first one is the dissociation region that contains the target gas, the electron gun, and the tellurium surface, and the second one is analysis region which contains quadrupole mass spectrometer. Methane is admitted to the dissociation region and evacuated from the analysis region, so there is a significant pressure drop across the aperture separating two chambers. The pressure inside the mass spectrometer and dissociation region was in the order of 10^{-5} and 10^{-3} Torr respectively. Methane is passed through the gas inlet which interacts with the electron coming from the electron gun in the dissociation region. Radicals produced by the electron methane collisions are converted to volatile telluride at the tellurium surface. The partial pressure of the telluride formed reflects the efficiency of conversion of radicals to telluride as well as the cross sections for radical production. Mass spectrometer measures the partial pressure of telluride in the lower-pressure region and is proportional to the telluride partial pressure in the higher-pressure region. Determination of the cross section for the production of a radical by electron impact by mass spectrometer signal rate mainly depends on its sensitivity, conductance of the aperture separating the high-pressure and low-pressure regions of the apparatus, radical-to- telluride conversion efficiency, the target gas pressure, the electron beam current, and the length of the cell.

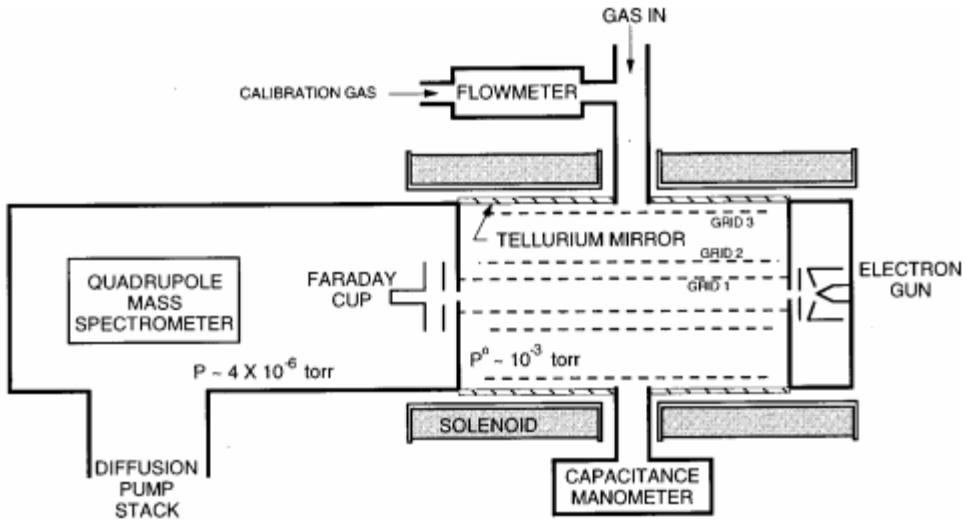

Fig.1.2. Schematic diagram of the apparatus for the measurement of neutral fragments of in Ref.12.

Electrons coming from the electron gun are accelerated into a beam that passes into the dissociation region, out through its exit aperture, through a secondary electron suppresser, and into a faraday cup. Faraday cup captures the electrons in order to measure the beam current. Methane is passed into the diffusion region by means of a diffusion pump. Tellurium is evaporated onto the inside surface of the cylinder in a separate apparatus to avoid contaminating the cell and the mass spectrometer with tellurium. The electron beam is surrounded by three concentric cylindrical grids. The innermost grid defines the field free region for the electron beam. The middle one is biased to prevent ions from escaping the collision region and impinging on the tellurium surface. The outermost grid is in contact with surface and thus defines the electrical potential of the tellurium surface.

Relative cross section for the production of CH_3 is measured by monitoring the intensity of the Te$(CH_3)_2^+$ peak in the mass spectrum. The neutral radical is mainly formed by any of the following two ways.

e +CH_4 $\rightarrow$ CH_3 + H + e neutral dissociation (n.d.)

e +CH_4 $\rightarrow$$CH_3$ + H^++2 e dissociative ionization (d.i.)

Since the data provided by the above two groups are not matching to each other, Casten Makochekanwa et al. [1] in 2007 made a new experimental method combining the crossed-beam method and the threshold ionization technique to study the neutral fragments produced by the electron CH_4 collision. Figure 1.3 is the schematic of the experimental set up. Their experimental set up consists of a primary electron gun, cross beam collision region, secondary ionizing electron gun, a quadrupole mass spectrometer (QMS) and the detection and counting electronics. The pressure in the collision region was fixed in the order of 7.5X 10^{-6} Torr. Electron CH_4 interactions in the collision region produce the neutral fragments as well as ionic fragments. The QMS was fixed perpendicular to the primary electron beam direction. Deflectors are inserted in between the QMS and collision region which help to select the neutral fragments and allow them to pass in the secondary ionization chamber. Neutral fragments in this chamber get ionized which are then detected by ion detection system. The number of radicals is directly proportional to the primary beam current, gas pressure in the collision region, the neutral dissociation cross section i.e. $\boldsymbol{\sigma}(CH_3)$, the impact energy and the integration time for pulse counting.

This experiment was done at low impact energies. The measurements made by this group agree with the measurements made by Moltagh and Moore [12]. But, they are significantly difference from the values of Nakano et al. [11]. This group measured the

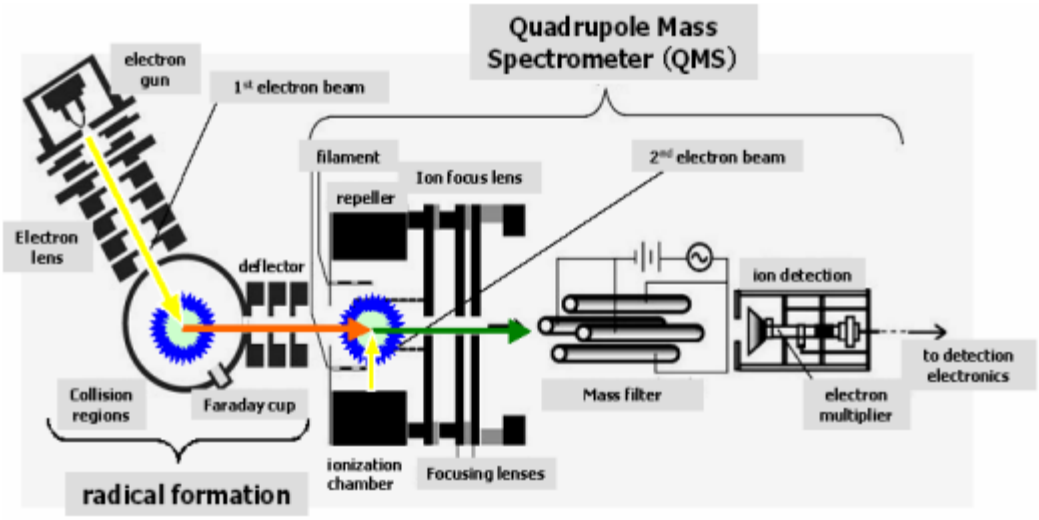

Fig.1.3. Schematic diagram of the experimental set up to measure the neutral fragments of CH_4 in Ref.1.

production cross section of CH_3 but did not measure the cross sections of the other neutral fragments like CH_2 ,CH, C and H.

There are very few theoretical measurements available for production cross section of neutral fragments. Daniel A. Erwin and Joseph A. Kunc in 2005 calculated the production cross section values for particular electron impact energy by using Robust Scaling Law [13]. In this method, authors used the values of ionization cross section to set the scaling law and hence to calculate the cross sections of neutral fragments. They considered three dissociation channels and four ionization channels. The same group in 2008 repeated the calculation using the same law with increased number (seven) of ionization channels [14]. Table 1.1 shows the cross section of CH_3, CH_2, and CH (in the order of $10^{-16}cm^2$) calculated by this group at an impact energy 100 eV in their second attempt. In the same table, available experimental cross sections at 100 eV are presented for comparison.

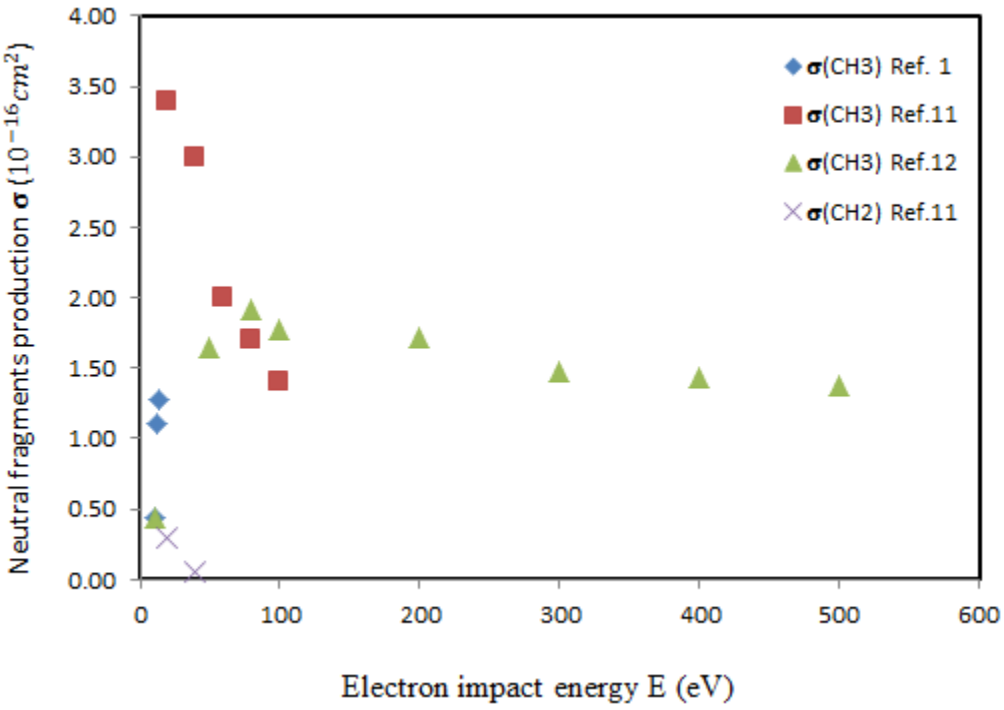

Fig.1.4. Available neutral fragment production cross section in the literature for CH_4 displayed as a function of electron impact energy E (eV).

Table 1.1. Dissociation cross sections of CH_3, CH_2 at electron bombardment energy 100 eV. Ref. [11] and Ref. [12] represent the experimental value and Ref. [14] represents the theoretical value.

Cross section	Experimental value		Theoretical value
	Ref.11	Ref.12	Ref.14
$\sigma(CH_3)$	1.40±0.21	1.78±0.10	2.22
$\sigma(CH_2)$	0.00		0.37
$\sigma(CH)$	0.00		0.18

As can be seen from table 1.1 two experimental results are not matching with each other for the production cross section of all three neutral. Also, none of the

experimental values with in their experimental uncertainties match with the theoretical values. It *is* evident here that there must be further experimental and theoretical work to determine the production cross sections of CH_3 at all electron bombarding energies. There is also the deficiency of the experimental and theoretical values of production cross sections like CH_2,CH, C and H.

CHAPTER TWO

Method of Determining Scattering Cross Section for Neutral Fragments (σ_n) in Electron CH_4 Collision

2.1 Cross Section of Different Process

A cross section is the effective area that governs the probability of some scattering or absorption event. Electron scattering cross section at particular energy measures the strength of the electron molecule interaction at that energy. When a beam of free electrons collide with molecules, there will be many interaction processes. These processes can be divided into two categories: inelastic collisions and elastic collisions. The process in which the bombarding electron loses a portion of its kinetic energy to the excitation degrees of freedom of the molecule is called inelastic collision. If there is no energy transformed to the motion of the target molecule, then this type of collision is termed as elastic collision. During this collision the electron loses some energy owing to momentum transfer, but this energy loss is proportional to the ratio of the mass of the electron to the mass of the target molecule, it is generally small compared with the energy lost to excitation of internal molecular degree of freedom. As a result of elastic and inelastic collisions, electrons scatter in all directions. The probability of scattering due to either of these two processes can be specified by their respective cross sections. So, the total electron scattering cross section (σ_t) can be expressed as a sum of elastic scattering cross section (σ_{elas}) and inelastic scattering cross section (σ_{inel}) as

$$\sigma_t = \sigma_{elas} + \sigma_{inel} \tag{2.1}$$

To understand the concept of the scattering cross section, let us consider a beam of electrons impinging on the target atoms as shown in the figure 2.1. The cross section d$\boldsymbol{\sigma}$ for electrons scattering into a solid angle dΩ can be defined as

— = ——————————————————————— (2.2)

the term $\frac{d\sigma}{d\Omega}$ is the differential scattering cross section, and is related to dN(θ), the number of particles per second scattered into a conical wedge define by θ and θ+dθ as

— —— . (2.3)

The element of solid angle dΩ= 2πsinθdθ, where θ is the angle between the scattered and incident directions, known as the scattering angle. So, the total scattering cross section can be defined as follows

$=2\pi\int_0^{\pi}\frac{d\sigma}{d\Omega}\sin\theta d\theta$. (2.4)

Elastic scattering may appear trivial as it involves no change in the internal energy state of the target molecule. However it does involve exchange of momentum between the colliding electrons.

As a result of the Inelastic collisions there are several phenomena like ionization, dissociation, excitation and vibration occur in the target molecule. Measurements of these phenomena can be expressed in terms of their respective cross section, ionization cross section (σ_i), dissociation cross section (σ_{diss}), electronic excitation cross section (σ_{elec}) and vibrational excitation cross section (σ_v) therefore,

$= \sigma_i + \sigma_{diss} + \sigma_{elec} + \sigma_v$. (2.5)

Combining equations (2.1) and (2.5), the total scattering cross section (σ_t) can be written as

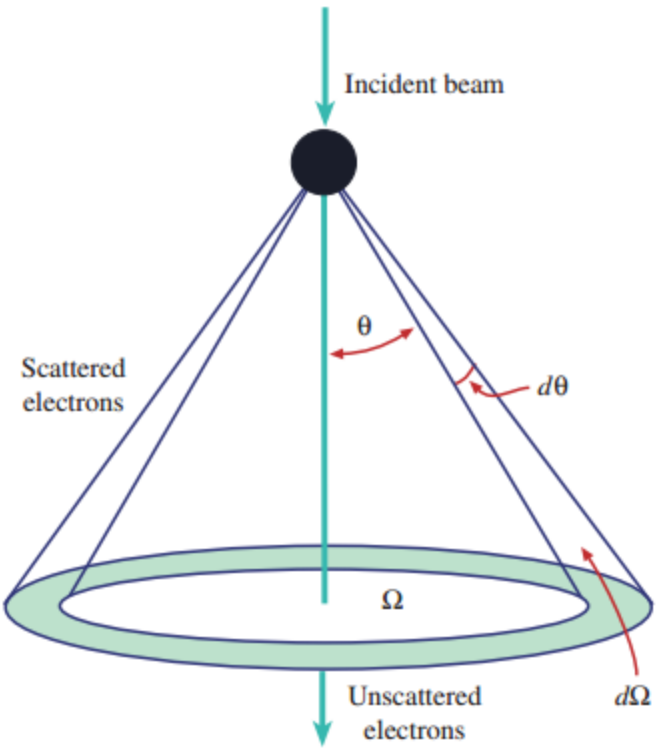

Fig. 2.1 Schematic diagram of a scattering

$$\sigma_t = \sigma_{elas} + \sigma_{\mathrm{i}} + \sigma_{diss} + \sigma_{elec} + \sigma_v. \quad (2.6)$$

Whenever energetic beam of electron collide with the target gas-phase molecule, provided the energy of this electron beam is greater than a critical value (Ionization energy), some atoms in the molecule will be ionized. Further increase of energy of the electron beam results in the increase of ionized species. These ionized particles may dissociate in several different channels, each of which gives characteristic ionized and neutral products as discussed in chapter one. If the energy of electron beam is lower than the ionization energy, those electrons may get into unoccupied molecular orbital (electron capture) that results in an unstable molecule. These molecules, also under go dissociation processes, which gives ions and neutral products.

2.2 Experimental Methods

Lambert-Beer law is used to determine the total scattering cross section, the most reliable cross section measurement, by measuring four quantities. They are the incident energy of the electrons, the fractional attenuation of the incident electrons due to scattering from the target molecule, the scattering length of target molecule through which the electrons must pass and the target gas density. The density of the target gas can be deduced from the ideal gas law through the measurements of the target gas absolute temperature and pressure. If we suppose the uniform temperature and pressure throughout the gas, the Lambert-Beer law can be expressed as

$$\text{Ln}\left(I_0/I\right) = \left(\sigma_t \text{L}/kT\right) \text{P}. \tag{2.7}$$

Where P is the pressure of the target gas, L is the scattering length through which the electrons travel, k is the Boltzmann's constant, T is the absolute temperature of the target gas, I_0/I is the fractional attenuation of the incident electron beam. In order to determine the total electron scattering cross section, it is necessary to design the experiment for the measurement of fractional attenuation of an electron beam due to scattering from the target molecule as a function of the target molecule pressure and electron beam energy [15]. A logarithmic plot of the fractional beam attenuation versus the pressure will be produced for each of the energy from the experimental results, and the slope of the resulting graphs deduced from the linear least squares fit. By knowing the absolute temperature and scattering length of the target gas, the total electron scattering cross section of the gas will be determined from these slopes by using the Lambert-Beer law.

a. Total Scattering Cross Section

There are two experimental methods to find the total scattering cross section (σ_t), Ramsauer technique and Linear Transmission Technique. The Ramsauer technique uses a uniform magnetic field oriented transverse to the plane of motion of the electron beam. The photo electrically emitted electrons are accelerated, and constrained to follow a circular path by means of a uniform magnetic field. The slits used in the apparatus as shown in the figure 2.2 help to collimate the beam and select a narrow energy spread. The current entering to the chamber B is the sum of the currents to chamber B and C. The fraction of current that reaches to the chamber C can be estimated by the following relation

$$I_C = (I_B + I_C)\, f e^{-\sigma n l} \qquad (2.8)$$

Here, f is fraction of sum of total current of chamber B, l is path length in chamber B, n is the number of target molecules per unit volume and σ is the total scattering cross section.

Linear transmission technique is the modified form of the Ramsauer method and being used in the present time. It consists of an electron gun, a gas cell and electrostatic energy analyzer. Figure 2.3 shows the experimental set up for this technique. A mono energetic electron beam of known intensity (I_0) is passed through the gas cell of known gas pressure (P) and the attenuated current intensity (I) is measured using the electrostatic energy analyzer. The total cross section is determined by studying the variation of attenuated current intensity as a function of target gas pressure.

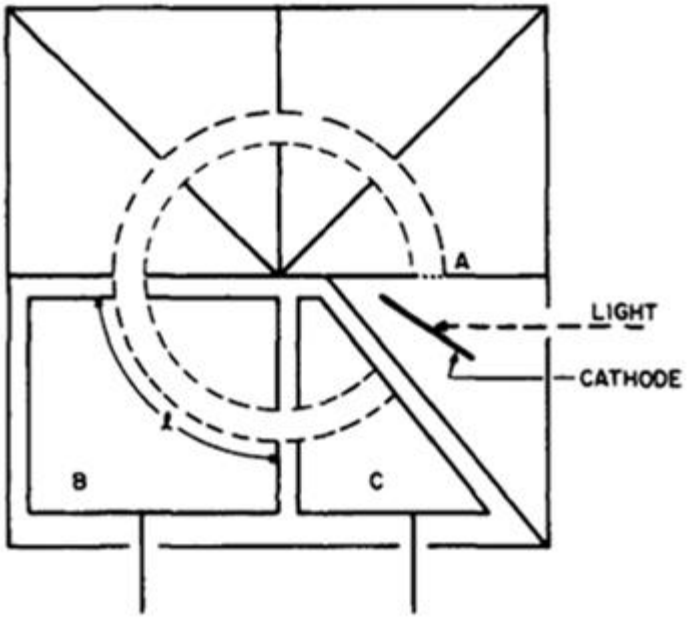

Fig. 2.2. Ramsauer apparatus for the measurement of total scattering cross sections for electrons in gas. Electrons are liberated photo electrically from the cathode, accelerated to the gridded aperture A, and then travel in a circular path in a uniform magnetic field.

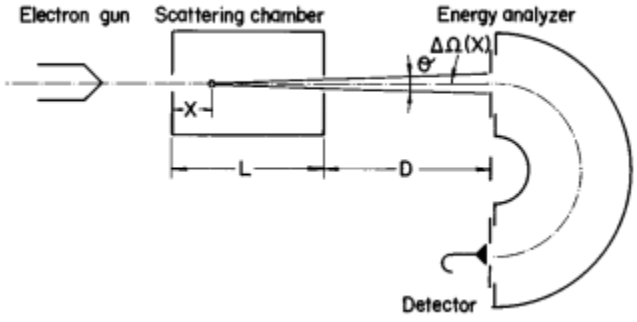

Fig. 2.3. Schematic of the experimental set up for the linear transmission technique used in Ref.16.

b. Elastic Scattering Cross Section

Electron Scattering Spectrometer is used to study the elastic scattering of electrons by molecules. The experimental set up is shown in figure 2.4. It consists of an electron monochromator, an electron energy analyzer, a target gas cell, and peripheral electronic devices [17]. The vacuum chamber is evacuated to about 10^{-8} Torr. Electron monochromator, an electron energy analyzer and target gas cells are placed in vacuum chamber. It is lined with magnetic shielding material to reduce the magnetic field to few milli Gauss (mG). Collimation, transport and energy selection of electrons are usually achieved by electrostatic techniques.

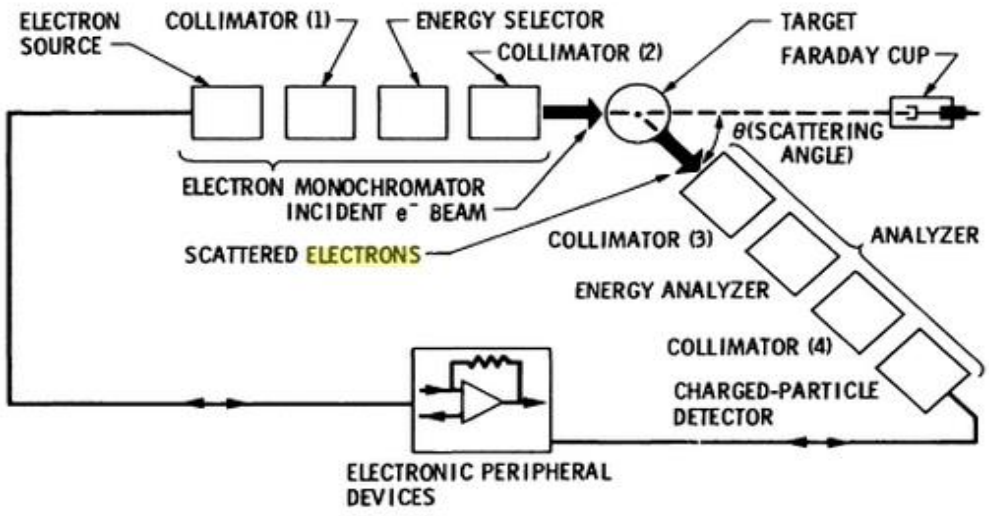

Fig. 2.4. Schematic for experimental set up of elastic scattering cross section in Ref.17.

c. Inelastic Scattering Cross Section

For the measurement of inelastic scattering cross section, one needs to measure the ionization cross section, dissociation cross section, electronic excitation cross section, vibrational cross section and neutral production cross section. The final products of

ionization and dissociation process are mainly ions. In many experiments, the cross sections of these processes are measured as one cross section, the ion production cross section. Most of the values of ion production cross sections in literature are found as a total ionization cross section. K. Gluch et al in 2003 [18] measured the ion production cross section of CH_4. The experimental set up is shown in the figure 2.5. It consists of an electron gun, a scattering chamber, deflector plates and detector. A well collimated beam of electron impacts the target gas (CH_4). The ions produced by electron- CH_4 collision are then passed through the deflector plates. After passing through the magnetic field followed by an electric field, the ions are detected by a secondary electron multiplier.

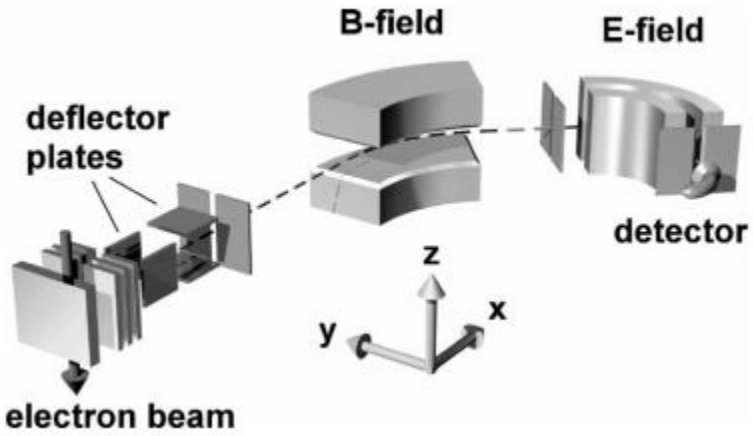

Fig. 2.5. Schematic of the experimental set up to measure the total ion production cross section in Ref.18.

S. Mondal, and R. Shankar [19] in 2006, performed an experiment to measure the total ion production cross section at different electron impact energies. The experimental set up is shown in the figure 2.6. This experiment is based on crossed-beam method. It consists of an electron gun, a scattering chamber, a channel electron multiplier (CEM) and a faraday cup. A mono energetic beam of electrons coming from the electron gun

interact with the cross-beamed target gas. The collisionally induced charged ions produced were extracted in a time of flight (TOF) spectrometer.

Though the experimental values of vibrational cross section and electronic excitation cross section are very small, they are explained in this section briefly for the completion of all experimental cross section measurements. Vibrational excitation cross sections are the least known quantities in electron molecule impact cross sections. Being very small, in most of the cases these are ignored. A schematic diagram of the apparatus used for the measurement of the vibrational excitation cross section [20] is given in figure 2.7. The apparatus consists of two chambers, upper chamber and lower chamber. These two chambers are pumped differentially to maintain a low background pressure in the lower chamber. The upper chamber consists of the source (CH_4). The lower chamber consists of the rotable electron beam source (E) and a fixed electron detector system (F). The electron beam source consists of an electron gun, two lenses and two electron beam detectors. Detector system consists of two electrostatic energy analyzers placed in series, two electron lenses and a channel electron multiplier. The vertically collimated CH_4 beam from the source enters the lower chamber through a double skimmer located between the two chambers. The incident electron beam of a given energy intersects with the collimated neutral beam in the interaction region. The scattered electrons from the methane beam at a given angle are detected by the channel electron multiplier after energy analysis. Thus, the energy loss spectrum of the scattered electrons is obtained at a given scattering angle at incident energy.

There are no experimental measurements found in the literature for the measurement of the electronic state excitation cross section (σ_{elec}). By knowing the

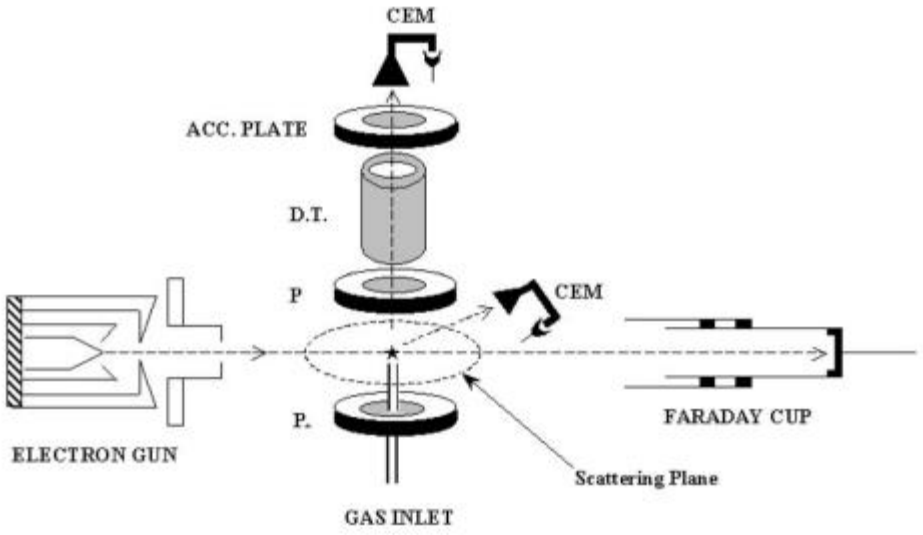

Fig. 2.6. Schematic of the experimental set up for the total ion production cross section measurement in Ref. 19. P; parallel plates, and D. T.; drift tube.

values of scattering cross sections for total (σ_t), ion production (σ_{i}), elastic (σ_{elas}) and the vibration (σ_v) at the particular electron impact energy, the value of electronic state excitation cross section (σ_{elec}) can be predicted easily by using following relation

$$\sigma_{elec} = \sigma_t - \sigma_{\mathrm{i}} - \sigma_{elas} - \sigma_v \ . \qquad (2.9)$$

No absorptions or emissions of the dissociating states of CH_4 are observed. So, the total electronic excitation cross sections should represent to a very good approximation the cross section for dissociation of CH_4 into neutral fragments.

Values of the vibrational cross section and the electron excitation cross section in case of electron impact CH_4 are very small and we neglect them while computing the scattering cross section of the neutral fragments. If one knows the value of total scattering cross section, elastic scattering cross section and the ion production cross section, one can estimate the value for the production cross section of the neutral fragments by using the expression as

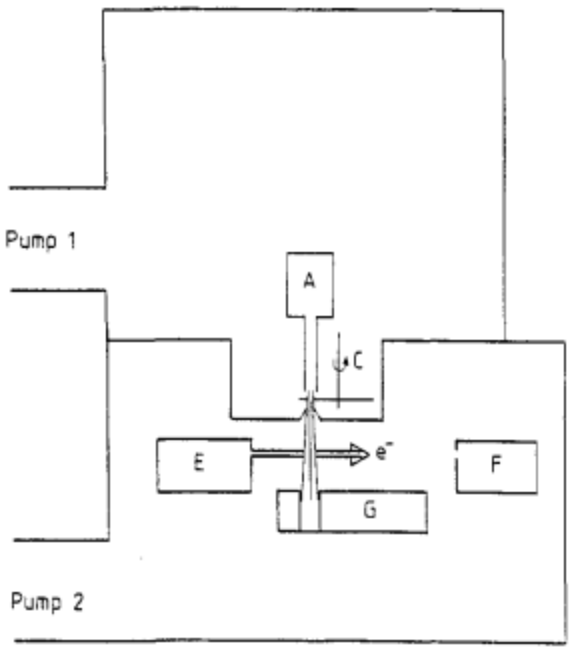

Fig .2.7. Schematic of the experimental set up for vibrational excitation cross section measurements used in Ref. 20. A, CH_4 beam source; C- chopper; E- electron beam source, F-electron detector and G- mass spectrometer.

$$\sigma_n = \sigma_t - \sigma_{elas} - \sigma_i \ . \tag{2.10}$$

Estimated values for the neutral production cross section by using the existing experimental cross sections of CH_4 will be presented next.

2.3 Estimation of σ_n By Using Existing Data

If one knows the values of different cross sections in equation (2.10), with the exception of the cross section of neutral fragment production (σ_n), then those could be used to predict σ_n. In the present section, existing data of the total scattering cross section (σ_t), ion production cross section (σ_i) , and elastic scattering cross section (σ_{elas}) are used to predict the production cross sections of neutral fragments at electron impact energies; 100-eV, 200-eV, 300-eV, 400-eV, and 500-eV. These energies are selected here

because many experimental groups have reported σ_t, σ_i, σ_{elas}, σ_v, σ_{elec}, σ_{inel}, σ_{diss} at these energies or closer energies. In the case of existing data which are at energies closer to 100-eV, 200-eV, 300-eV, 400-eV, and 500-eV, the interpolated and extrapolated values are used as explained in each section.

a. Existing Values for

Antonio Zecca et al. in 1991 [21] measured the total cross sections for electron scattering on CH_4 molecules in the impact energy range 1- 4000 –eV. An electrostatic analyser had been used to select the electron beam for energies lower than 75-eV while a modified Ramsauer- type spectrometer had been used for energies higher than 75-eV. G.Garcia, and F. Manero in 1997 [22] predicted the total scattering cross section of for different electron impact energies; 1- 5000-eV, by using an analytical formula. G. Gracia and P. Manero in 1998 [23] measured the total scattering cross sections of experimentally with in the electron impact energy range 400- 5000-eV. In 2002, W.M. Ariyasinghe and D. Powers [24] measured the electron scattering cross section of CH_4 for the electron impact energies 200-1400- eV. This experiment was based on the linear transmission technique. Fig. 2.8 displays the values of total scattering cross sections of CH_4, obtained by these groups. These cross sections are within the experimental uncertainty of ± 3%. The measurements given in Ref. 24 is in close agreement with the values given in references 21-23. Therefore, in the present section, only the values of total scattering cross section of CH_4 given in reference 24 are used for the prediction of σ_n. The figure 2.8 provides the total scattering cross section for all impact energies except for 100 –eV in reference 24. The value of total scattering cross section for 100 –eV can easily be predicted from the graph by extrapolating it.

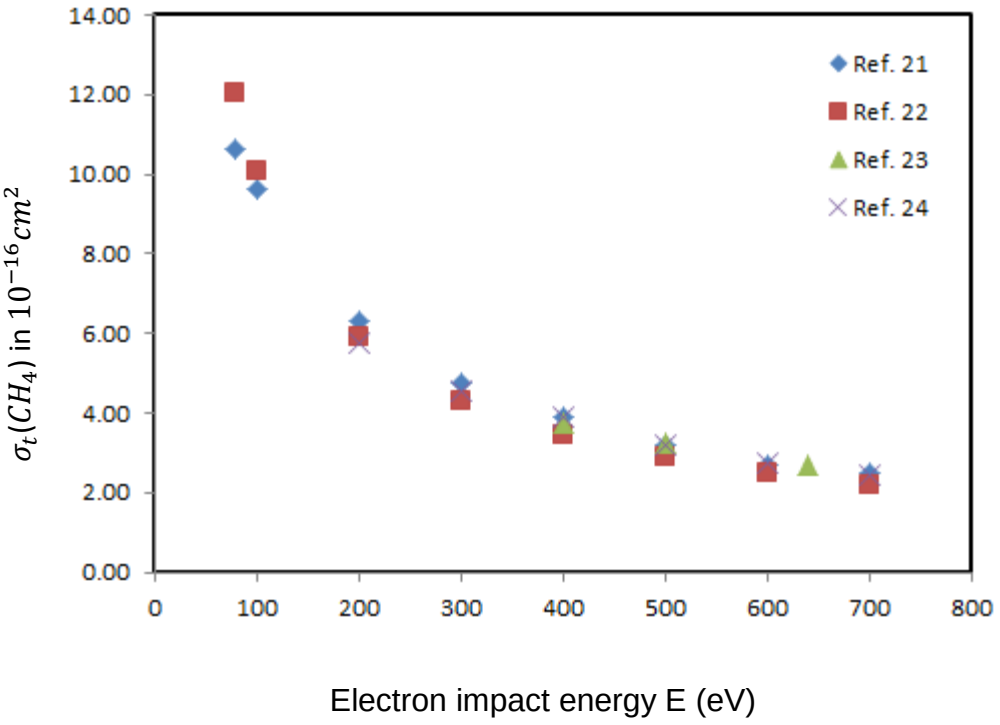

Fig. 2.8. The experimental total scattering cross sections σ_t of CH_4 reported by different experimental groups.

b. Existing Values for σ_{elas}

There are few measurements of elastic scattering cross sections (σ_{elas}) in the literature for CH_4 at different energy ranges. However, only one experimental group has reported σ_{elas} for CH_4 in the energy range (100-500-eV) as interested in this work. The results obtained by the T Sake et al are in the close agreement with those of previous results. T Sake et al in 1989 [25] performed an experiment to measure the elastic scattering cross section of methane (CH_4) , and two other gases. This experiment was based on crossed-beam method. Figure 2.9 displays the values of elastic scattering cross section of CH_4 for different impact energies reported in this work. These cross sections are within the experimental uncertainty of ± 10%. Elastic scattering cross section of CH_4

for the energy 400-eV is predicted by interpolating the graph, which will be used later to compute the value of σ_n.

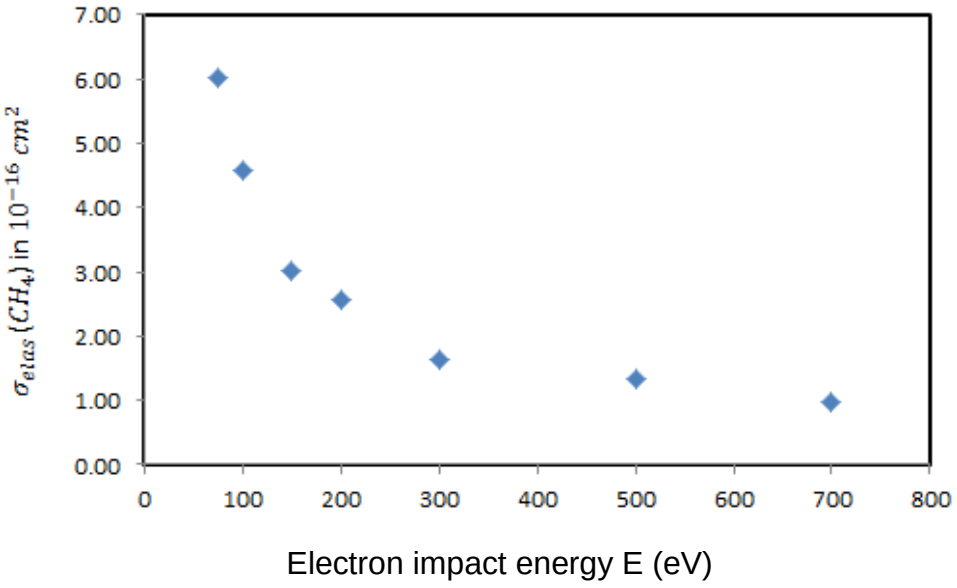

Fig. 2.9. Variation of elastic scattering cross sectionσ_{elas} (experimental) with electron impact energy. This figure will be used to interpolate the elastic scattering cross sections of the unknown energies.

c. Existing Values for σ_i

Ion production cross section (σ_i) is the sum of cross sections of all charged fragments produced during the electron molecule collisions. In 1965, Donald Rapp and Paula Englander-Golden [26] measured the ion production cross section of several gases including CH_4 for the electron impact energies within the range 10-1000-eV. These measurements have ± 2% experimental uncertainty. In 1984, H. Chatham, D. Hils. R. Robertson and A. Gallagher [27] measured the ion production cross section of CH_4 and other three molecules, in the electron impact energy range 15-400-eV. These cross sections are within the range of ±14% experimental uncertainty. In 1987, OJ Orient and

SK Srivastava [28] measured the ion production cross section of different molecules including CH_4. These cross sections measurements were done within the impact energy range of 10-510-eV with the experimental uncertainty of ± 1%. In 1994, H Nishimura and H Tawara [29] measured the ion production cross section of CH_4 along with other different molecules in the electron impact energy range threshold to 3000-eV. These measurements have ± (0.4-5.9) % experimental uncertainty at different energies. Though the values given by these groups are very close to each other at some of the impact energies, all the values obtained from these groups are used for the prediction of σ_n for the energies interested in this work. One can easily compare the ion production cross sections σ_i given by these groups which are displayed in the figure 2.10.

d. Estimation of σ_n

It shows that different groups have measured the cross sections of different types at particular electron impact energy. Displayed graphs [Fig. 2.3 a-c] presented above help to estimate the values of these cross sections for different impact energies. Table 2.1 shows the estimated values of the production cross sections of neutral fragments by using the existing data of different cross sections of different processes given in the relation 2.10 ; $\sigma_n = \sigma_t - \sigma_{elas} - \sigma_{ion}$. The numbers in the parentheses and square brackets are estimated values obtained by extrapolation and interpolation of the graphs respectively.

From table 2.1 it is clear that the range of the values of σ_n obtained by using the different cross sections of different groups agree with in the experimental uncertainties

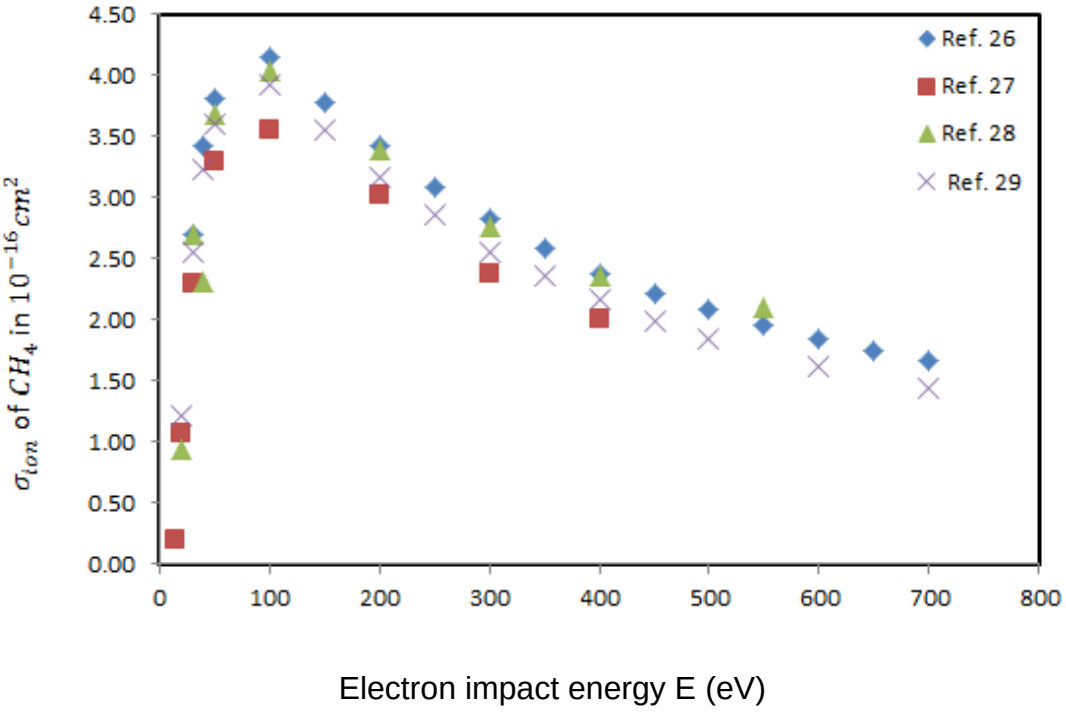

Fig. 2.10. The ion production cross sections (σ_{ion}) reported by different experimental groups (references 26-29) in the electron energy range 0- 700 eV.

for all of the impact energies. One can select the best combination of groups for the particular energy from this table which helps to design the best experimental set up for the future measurements of the values of σ_n . As can be seen from these estimations, it is clear at 100 –eV σ_n could be in the range of zero to $2.12X10^{-16}cm^2$. Further the lower limit of σ_n is zero for all of these energies while the upper limits are $0.74X10^{-16}cm^2$, $0.96X10^{-16}cm^2$, $0.73X10^{-16}cm^2$, $0.22X10^{-16}cm^2$, respectively, for 200-eV, 300-eV, 400-eV, and 500-eV. Here, the lower limit of σ_n zero means it is in the order of low $10^{-17}cm^2$. Since the reported cross section carry certain experimental uncertainties, those propagate into the σ_n lower limit estimation making it zero or negative.

Table 2.1. Estimated values of σ_n by using existing cross sections. The values obtained by extrapolation of the graphs are in parentheses whereas the values in the square brackets represent the values obtained by the interpolation of the graphs.

Electron impact energy E (eV)	Ref.	Total scattering cross section σ_t ($10^{-16}cm^2$)	Ref.	Elastic scattering cross section σ_{elas} ($10^{-16}cm^2$)	Ref.	Ion production cross section σ_i ($10^{-16}cm^2$)	Estimated value for σ_n ($10^{-16}cm^2$)
	24	(9.50) ±0.31	25	4.59±0.45	29	3.92±0.11	0.99±0.55
100	24	(9.50) ±0.31	25	4.59±0.45	28	4.04±0.08	0.87±0.55
	24	(9.50) ±0.31	25	4.59±0.45	27	3.55±0.53	1.36±0.76
	24	(9.50) ±0.31	25	4.59±0.45	26	3.65±0.07	1.26±0.55
	24	5.78 ±0.20	25	2.56 ±0.23	29	3.17 ±0.04	0.05 ±0.30
200	24	5.78 ±0.20	25	2.56 ±0.23	27	3.02 ±0.45	0.20 ±0.54
	24	5.78 ±0.20	25	2.56 ±0.23	26	3.00 ±0.06	0.22 ±0.31
	24	4.55 ±0.18	25	1.63 ±0.14	29	2.55 ±0.05	0.37 ±0.23
	24	4.55 ±0.18	25	1.63 ±0.14	27	2.37 ±0.35	0.55 ±0.41
300	24	4.55 ±0.18	25	1.63 ±0.14	26	2.48 ±0.04	0.44 ±0.23
	24	4.55 ±0.18	25	1.63 ±0.14	28	2.76 ±0.05	0.16 ±0.23
	24	3.90 ±0.07	25	[1.50] ±0.15	29	2.17±0.04	0.23 ±0.17
400	24	3.90 ±0.07	23	[1.50] ±0.15	28	2.36±0.04	0.04 ±0.17
	24	3.90 ±0.07	23	[1.50] ±0.15	27	2.01±0.04	0.39±0.34
	24	3.90 ±0.07	23	[1.50] ±0.15	26	2.09±0.04	0.31±0.17
	24	3.20 ±0.13	23	1.33 ±0.13	29	1.85 ±0.06	0.02 ±0.19
500	24	3.20 ±0.13	25	1.33 ±0.13	26	1.82 ±0.03	0.05 ±0.18
	24	3.20 ±0.13	25	1.33 ±0.13	28	2.10 ±0.04	0.04 ±0.18

2.4 Determination of σ_n By Theoretical Methods

There are very few theoretical methods found in the literature for the determination of production cross section of neutral fragments of CH_4 along with other hydrocarbons. R.K. Janev and D. Rieter in 2002[30] established an analytical formula to determine the total electron impact dissociation cross sections of CH_4 to neutral fragments (σ_{DE}^{tot}) as(y=1-4)

$$\sigma_{DE}^{tot}\ (CH_y) = 34.6[1+0.29y](1-\frac{E_{th}}{E})^{3.0}\ \frac{1}{E}\ln(e+0.15E)X10^{-16}cm^2\ . \quad (2.11)$$

In this equation, E_{th} and E are threshold and collision energy respectively in eV, and e = 2.71828..., the basis of natural logarithm. The equation 2.11 shows the linear relationship of σ_{DE}^{tot} with the number of hydrogen atoms in CH_y. Therefore, this relation can also be converted into a new form 2.12 which is used to determine the particular neutral dissociation channel (A) of CH_y as

$$\sigma_{DE}(^{A}/_{CH_y}) = R_{DE}(^{A}/_{CH_y}) \bullet \sigma_{DE}^{tot}\ (CH_y)\ . \qquad (2.12)$$

Where, $R_{DE}(^{A}/_{CH_y})$ is the branching ratio. This group had reported the values for threshold energies E_{th}, and the branching ratios which are presented below in table 2.2. By the use of equation 2.11-2.12 and the table 2.2, one can easily compute the cross section of neutral fragments. As an example, the value of production cross section of CH_3 is calculated when the methane is impacted by 100 eV electrons. In the notation given in equations 2.11 and 2.12, this cross section is $\sigma_{DE}^{tot}(\frac{A}{CH_y})$. By using A = CH_3, y = 4, R_{DE} = 0.760, and E_{th}= 6.6 eV in these equations, one can calculate the production cross section of CH_3 as 1.31X$10^{-16} cm^2$. In this calculation, R_{DE} and E_{th} are taken from table 2.2 (1^{st}line). The production cross sections of all possible fragments of CH_4 predicted from this formula at different electron impact energies interested in this work are displayed in the figure 2.11.

In 2005, Daniel A. Erwin and Joseph A. Kunc [13] established a Robust Scaling Law to determine the production cross sections of neutral fragments from the CH_4 by the impact of electrons at different energies. This law is based on the ratios of particular neutral fragment with the total neutral fragments and the particular ion production with the total ion production. There is a correspondence between these two ratios. By

Table 2.2. Values of threshold energies and branching ratios for different dissociation channels as reported by Janev and Rieter[30].

Reaction Channel	R_{DE}	E_{th}(eV)
e + CH_4 → CH_3 +H + e	0.760	6.6
→ CH_2 + H_2+ e	0.144	7.0
→ CH + H_2 + H + e	0.073	12.0
→ C + 2H_2+ e	0.023	10.6
e + CH_3 → CH_2 +H + e	0.83	6.9
→ CH + H_2+ e	0.14	7.2
→ CH + 2H + e	0.02	12.4
→ C + H_2+ H + e	0.03	10.6
e + CH_2 → CH +H + e	0.90	6.4
→ C + H_2+ e	0.08	6.6
→ C + 2H + e	0.02	10.4
e + CH → C +H + e	1.0	5.3

observation and analysis of the relationships between the available data on ion production cross sections and the neutral production cross sections, they have defined the following ratios to develop a mathematical expression for the neutral production cross sections as

$$\lambda_{mn}(E) = \frac{\sigma_m(E)}{\sigma_n(E)} \quad . \tag{2.13}$$

$$\lambda_{di}(E) = \frac{\sigma_d(E)}{\sigma_i(E)} \quad . \tag{2.14}$$

Where, E= electron impact energy, σ_m (m=1, 2, 3) refers to the production cross sections of CH_3, CH_2 and CH respectively, σ_n(n=5, 6, 7) refers to the production cross sections of CH_3^+, CH_2^+ and CH^+ respectively, σ_d is the total production cross sections of neutral

fragments and σ_i the total ion production cross sections. Therefore, the three different values of λ_{mn} are

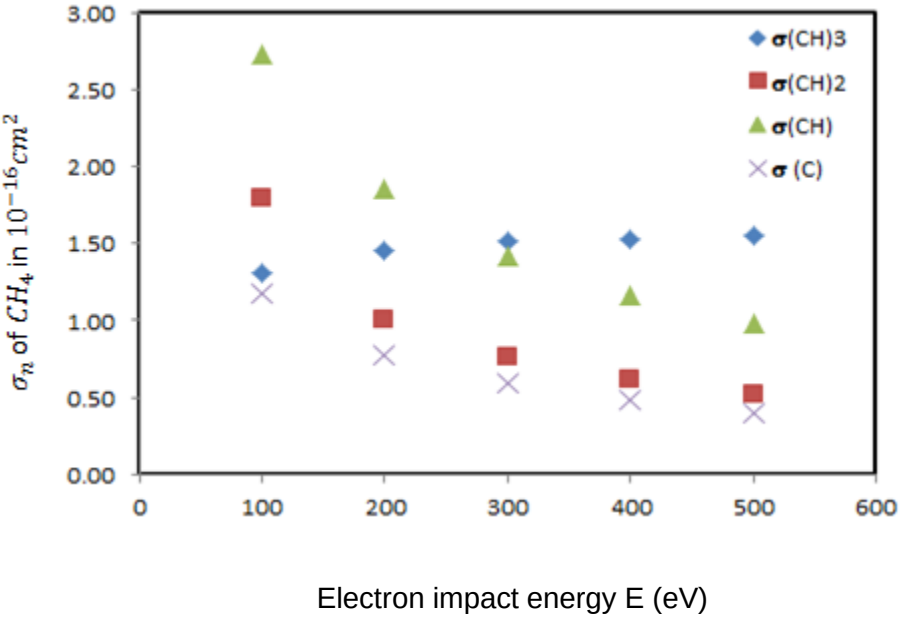

Fig. 2.11. Variation of production cross sections of the different fragments produced from with the electron impact energy. These cross sections are calculated using the analytical expression 2.11 in reference 30.

$$= \frac{\quad}{\quad}, \qquad = \frac{\quad}{\quad} \text{ and } \qquad = \frac{\quad}{\quad} . \tag{2.15}$$

One can find the experimental values of production cross sections of and in the literature. Therefore, it is easy to get the value of . T. Shirai, et al. [31] presented the values of the production cross sections of , and at different electron impact energies. But due to the scarcity of the values of and $\sigma_3(E)$ in the literature, it is difficult to determine the values of $\lambda_{26}(E)$ and . This group tried to find a scaling law that is suitable to get $\lambda_{26}(E)$ and and hence the values of

$\sigma_2(E)$ and $\sigma_3(E)$. Using this approach, Daniel Erwin and Joseph A. Kunc [13] developed a new relationship that is valid up to 500-eV to predict $\sigma_2(E)$ and $\sigma_3(E)$. The new relationships are

$$\sigma_m(E) = \sigma_n(E) \left[\frac{\sigma_d(E)}{\sigma_i(E)} + \alpha_{mn} d_{15}(\mathrm{E}) \right] \quad (2.16)$$

Where, $\alpha_{26} = 0.190$ and $\alpha_{37} = 0.042$

$$\sigma_d(E) = \frac{4.48\, X10^7\, (E')^{3.590} + 19.83\, (E')^{7.525}}{1.14\, X\, 10^{11} + 4.46\, X10^6\, (E')^{3.935} + (E')^{7.870}} \quad (2.17)$$

where, the value of $E' = E$- 4.51-eV

$$\sigma_i(E) = \frac{10.26 \ln E - 25.94}{E[3.77\, X\, 10^{-2} + (E-13)^{-0.906}]} \quad (2.18)$$

$$\sigma_5(E) = \frac{5.55\, X\, 10^{-2}\, (E')^{1.435}}{1 + 0.0257\, (E')^{1.509} + 2.59\, X\, 10^{-5}\, (E')^{2.635}} \quad (2.19)$$

where, $E' = E$- 14.24-eV

$$\sigma_6(E) = \frac{9.22\, (E')^{1.868}}{10^4 + 4.66\, (E')^{2.168} + 0.10\, (E')^{2.868}}\ , \quad (2.20)$$

where, $E' = E$- 15.20-eV

$$\sigma_7(E) = \frac{5.01\, X\, 10^{-3} (E')^{1.161}}{1 + 0.00117\, (E')^{1.831} + 1.19\, X10^{-6}\, (E')^{2.761}}, \quad (2.21)$$

where, $E' = E$- 24.14-eV, and

$$d_{15}(\mathrm{E}) = 0.4084 e^{-0.00093} E^{0.1241}. \quad (2.22)$$

In the equation 2.16, $\sigma_d(E)$, $\sigma_n(E)$, and $\sigma_i(E)$ are respectively the total cross section for the electron-impact dissociation of the CH_4 molecule into all neutral fragments, the cross sections for the ionizing processes for the production of three positive ions CH_3^+, CH_2^+ and CH^+, and the total cross section for the electron-impact ionization of the molecule into all charged fragments. The production cross sections of neutral fragments at the

impact energies interested in this work obtained from these relationships are displayed in figure 2.12.

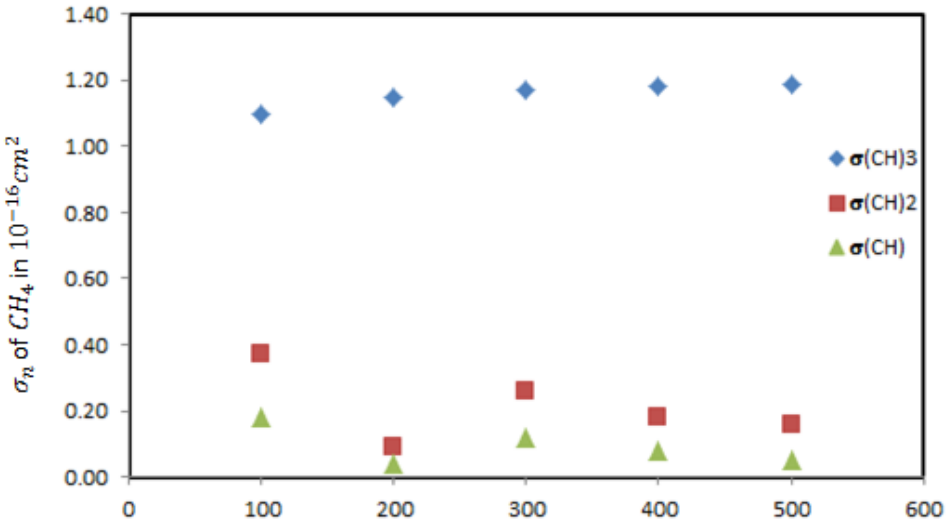

Fig. 2.12. The production cross sections of neutral fragments of CH_4 at different electron impact energies obtained by using the robust scaling law as explained in ther reference 13.

In 1998, G. Garcia and F. Manero [23] predicted the production cross section of neutral fragments produced from the methane by using the Born-Bethe approximation. In this method they presented the cross section for neutral fragment production as

$$\sigma_n = [28.3 \ln(\frac{E}{R}) + 6.93] \frac{R}{E} a_0^2 . \quad (2.23)$$

Where, E is electron impact energy in eV, R is Rydberg constant in eV, and a_0 is the Bohr radius.

One can compare the total production cross section of neutral fragments of CH_4 obtained by the above three theoretical methods. All of these methods do not provide the production cross section for a given neutral fragment through a given channel, but able to

predict the total value of σ_n. Total σ_n predicted by the above three theoretical methods are displayed in the figure 2.13 for comparison. As can be seen from this figure, none of the theoretical total neutral production cross sections agree to each other. The cross sections proposed in reference 23 are about 30% of those in reference 23 while those in reference 13 are about 60% of the reported cross sections in reference 30. Therefore, further work on this subject is required to determine the accurate values of the production cross sections of neutral fragments in CH_4.

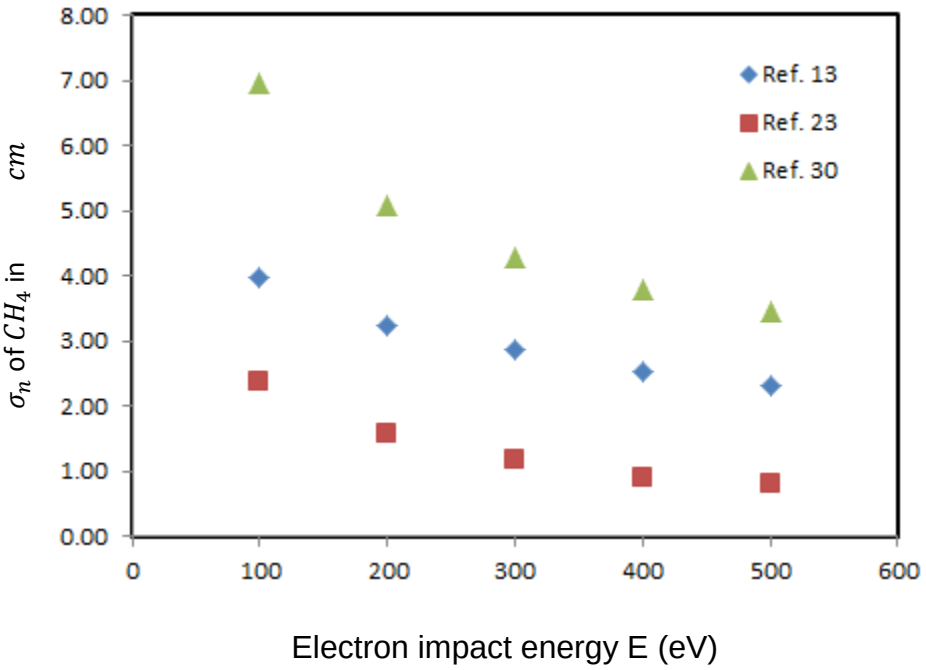

Fig. 2.13. The comparison of the total neutral production cross sections proposed by different theoretical groups.

CHAPTER THREE

Planned Experimental Set Up

3.1 Overview

The disagreement in the measurements of the production cross section of neutral fragments of CH_4 as seen in the chapter one section two and chapter two sections two and three demands the necessity of further research works in this field. A new experimental arrangement to measure the production cross sections of neutral fragments under the bombardment of energetic electrons will be discussed in this chapter. Figure 3.1 shows the schematic of the planned experimental arrangement. It consists of an electron gun, electrostatic lens system, pulsing valve, faraday cup, deflector, secondary electron source, ion repeller, time of flight mass spectrometer [TOF], ion accelerator, ion focusing lenses, and a micro channel plate detector [MCP detector]. These items are housed in a vacuum system that maintains the pressure of $3X10^{-7}$ Torr or better. The continuous beam of electrons will be generated from the electron gun. The electrostatic lens system helps to focus it at the center of the chamber, where it strikes the gas (CH_4) pulses coming from pulsing valve. Gas pulses and electron beam are in the cross-beam configuration. After the collision, different fragments of the CH_4 will be produced and those will move away from the interaction point. The electrostatic deflector which is in the path of fragments will deflect all ionic fragments while permitting neutral fragments to enter the secondary ionization chamber. A filament that emits threshold ionization energy electrons is positioned in the secondary ionization chamber. Distance L_0 in the figure 3.1 is the distance neutral fragments travel soon after their production at the primary interaction

point. After travelling the distance L_0, they will reach the point where the secondary ionisation occurs upon interaction with secondary electron beam. Thus produced ions will then be repelled away by the positive voltage on the repeller.

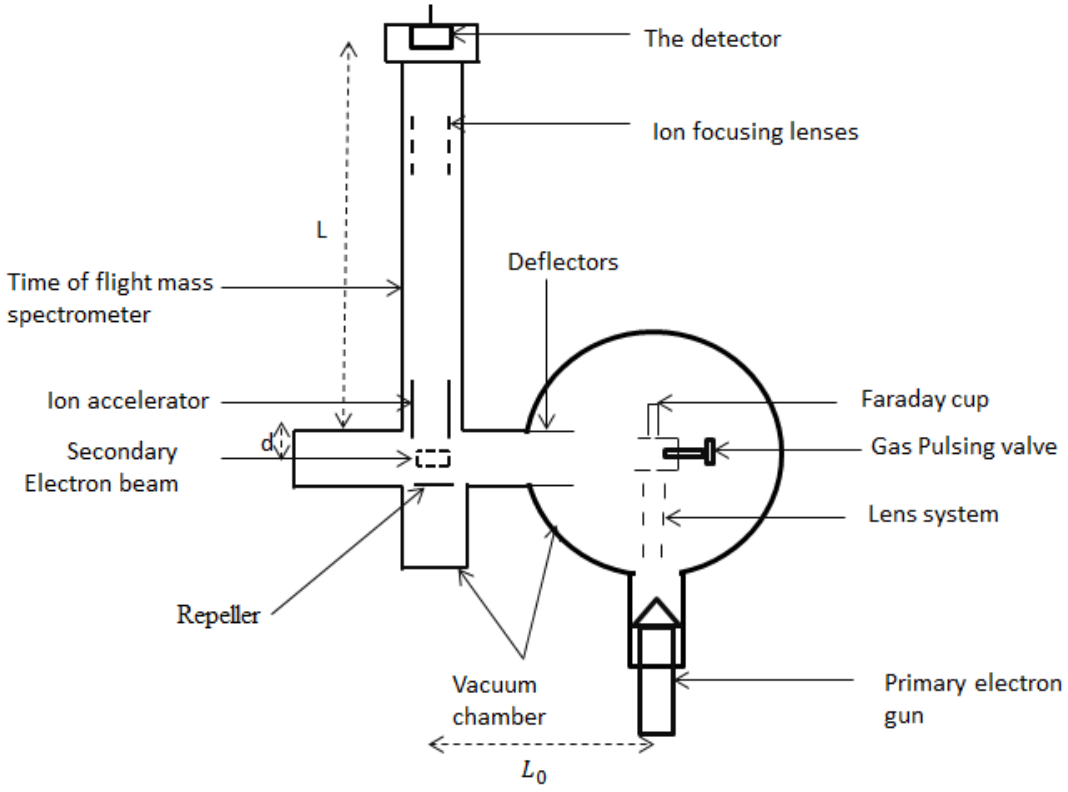

Fig. 3.1. Planned experimental set up for the measurement of the neutral fragments produced from CH_4. In the figure L_0= 66 cm, and L = 166 cm respectively.

After travelling the distance L_0, they will reach the point where the secondary ionisation occurs upon interaction with secondary electron beam. Thus produced ions will then be repelled away by the positive voltage on the repeller. There after these positive ions will be accelerated by the ion accelerator of the TOF mass spectrometer. The distance L in the figure is the distance that the ionized fragments should travel soon after the repulsion by

the repeller in the secondary ionization chamber. Since the different fragments are with different masses the time taken by each fragment to travel the distance L is different. Therefore, each of the ionized particles detected by the MCP can be distinguished on the basis of their arrival time to the detector. The major components of this experimental setup are explained as follows.

3.2 The Electron Gun

Electron gun provides a uniform electron beam. The energy of the electrons produced can be varied by the application of the voltage through the power supply unit. The schematic of the electron gun, electron path inside the electron gun and electrical connections are shown in the figure 3.2. The cathode is heated by the applied energy through the power supply unit. Therefore the electrons are given off from the surface of the cathode and it takes the path as shown in the figure 3.2 (C). The final energy gained by the electrons can be determined by knowing the difference between the potential set up of the power supply and the final potential (ground). Different energy range can be applied to the electron gun by using the energy power supply depending upon the electron gun.

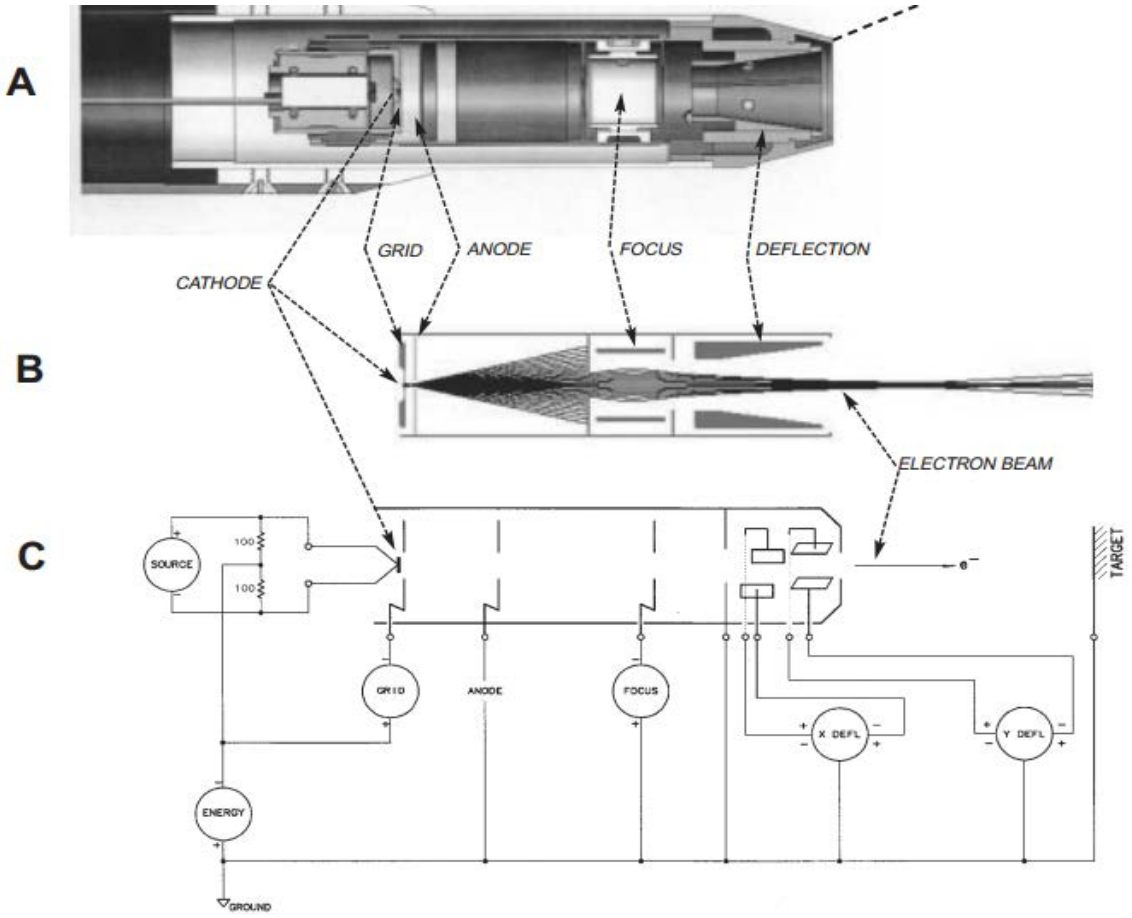

Fig. 3.2. The schematic of the electron gun, electron path inside the electron gun and electrical connections in the reference 32. In this figure; (A) a three dimensional cross sectional view (B) paths of the electrons in gun (C) a block diagram with the electrical connections of the power supplies and gun elements.

3.3 The Einzel Lens System

Electrostatic lenses are widely used to control beams of charged particle with various energy and directions. The lens systems can be operated to keep the image position constant. Einzel lens system is a kind of three-element lens in which the outer electrode are held at the same potential and beam focusing is achieved by varying the potential of the center electrode. The schematic of the einzel lens used in this lab is

shown in the figure 3.3. The focal distance of the lenses used is calculated by using the relation as

$$\frac{1}{P}+\frac{1}{Q}=\frac{1}{F} \quad . \tag{3.1}$$

Where, P is the distance between the lenses to the source of the electron gun, Q is the distance between the lens system to the electron-gas interaction point, and F is the focal distance. When parallel beams of electrons coming from the electron gun enter into the lens system they get focused at the primary interaction region as shown in the figure 3.3. Here, parallel beams of electron are coming, so object distance is considered as infinity.

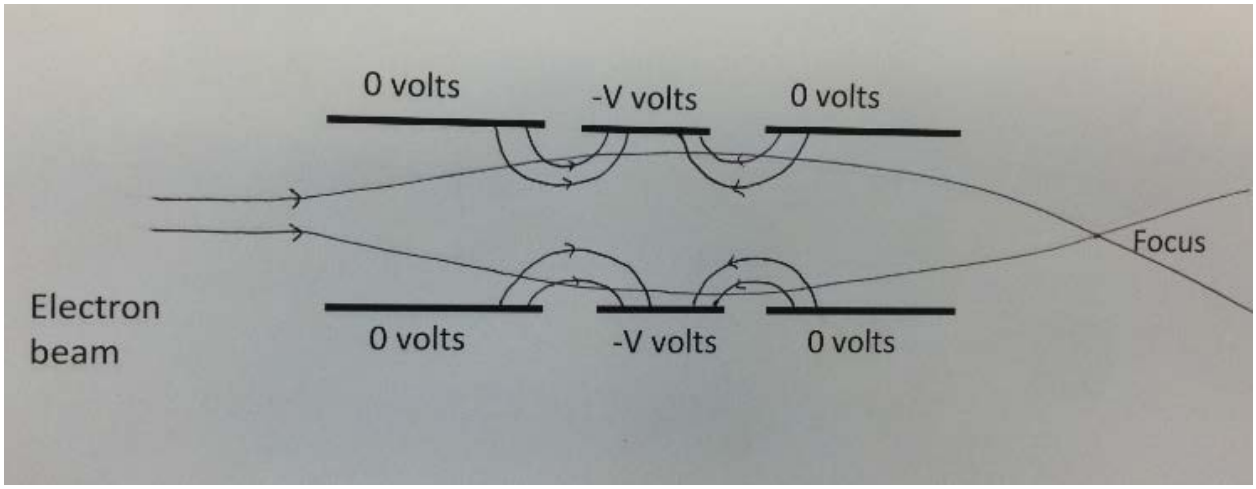

Fig.3.3. Schematic of cylindrical einzel lens in which diameter of the lens is 0.44 cm,gap between the lenses is 0.2cm, distance from first lens to the electron gun is 1.02 cm and the image distance (Q) is .55cm.

Therefore, the focal distance of the lens system is equivalent to the Q.

To get the focusing voltage of the lens for particular electron energy, several readings of the beam intensities are measured using faraday cup-pico ammeter combinations mounted at the exit port of the lens. Different voltages are applied on the central lens and the corresponding readings of faraday cup-pico ammeter combination are

taken. At particular voltage on the lens, the reading on the Pico ammeter becomes maximum. On the basis of these readings a graph of electron energy versus focusing voltage is plotted. This plot is displayed in the figure 3.4. As can be seen from the figure, focusing voltage has a linear relationship to electron energy. These voltages are the required focusing voltages that should be applied to the lens during the experiment.

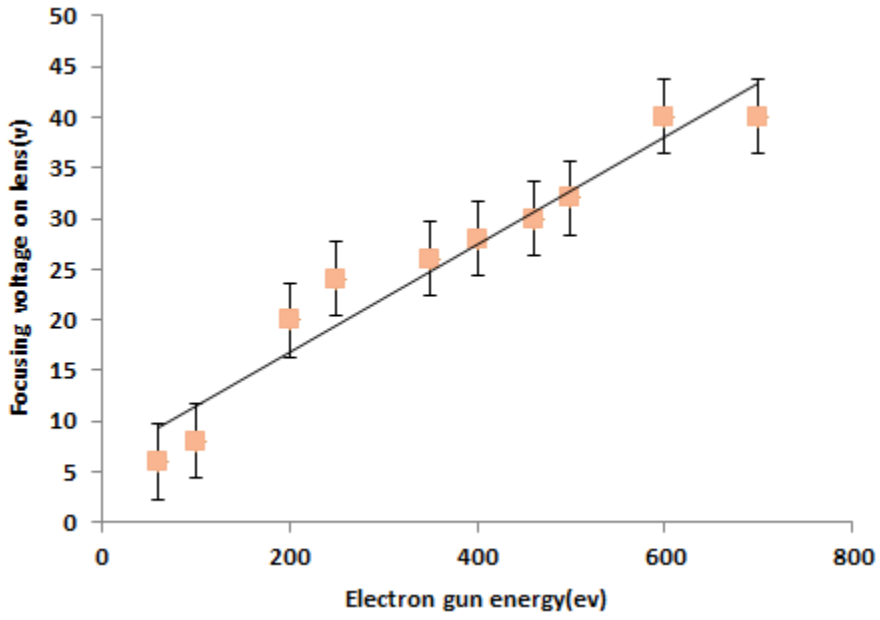

Fig. 3.4. Variation of focusing voltage on lens versus the electron energy.

3.4 The Pulsing Valve

Pulsing valve is used to supply the target gas to the collision region of the vacuum chamber in the certain time interval. It produces the repeatable pulses at ultra-high speed and requires no pressure to operate it. It can work in the temperature range -40^0C to 200^0C. The diameter of the orifice of the pulsing valve used in this experimental set up is

1.0 mm. This valve is operated by 12V pulse generated from a pulsing power supply. Power supply on the Pulsing valve is controlled by lab view programming.

3.5 Time of Flight Mass Spectrometer

The flight time for each singly charged mass is unique upon accelerated by a constant retarding potential. The time-of flight mass spectrometers are based on a simple mass separation principle that depends on the flight time of each individual mass. Particles follow the path as shown in the figure 3.1. Flight time for any particle is the time taken by it to travel the distance from the collision region to the detector. Therefore, to get the total time of flight, first, one should calculate the time required for the particle to travel the distance L_0 , second time taken by the particle to travel the distance from secondary ionization region to the accelerating region (d), and finally the distance L. From the kinetic theory of gas the pressure inside the chamber is

$$P = \frac{1}{3} nmv^2 \ . \qquad (3.2)$$

Where, n is the number of particles per unit volume v is the velocity of the particle and m is the mass of the particle. From the ideal gas law

$$P = k_B T \ . \qquad (3.3)$$

In which, k_B is the Boltzmann's constant = $1.380\text{X}10^{-23} JK^{-1}$.

Combining relations (3.2) and (3.3), the expression for the velocity now becomes

$v = \sqrt{\frac{3k_B T}{m}}$, where T is the room temperature. (3.4)

Therefore, the time (t_1) taken by the particle to travel the distance L_0 is

$$t_1 = L_0 \sqrt{\frac{m}{3k_B T}} \ . \quad (3.5)$$

When the particle reaches to the secondary ionization region, it gets ionized by threshold energy electrons. If the electric field of the retarding potential is E, the time (t_2) taken by the particle to reach to the accelerating region from the secondary ionization region is

$$t_2 = \sqrt{\frac{2md}{eE}} \ . \quad (3.6)$$

Where e is electronic charge.

In the accelerating region it gets accelerated by the potential V. Therefore, the kinetic energy (KE) of the particle is

$$\text{KE} = eV = \frac{mv^2}{2} \quad . \quad (3.7)$$

If t_3 is the time taken by the particle to reach to the detector, then

$$t_3 = \frac{L}{v} \quad . \quad (3.8)$$

Plugging the value of v from (3.7) into (3.8), the expression for t_3 now becomes

$$t_3 = L\sqrt{\frac{m}{2eV}} \ . \quad (3.9)$$

Therefore, the total time taken by the particle to reach to the detector is

$$t = t_1 + t_2 + t_3$$

$$= L_0 \sqrt{\frac{m}{3k_B T}} + \sqrt{\frac{2md}{eE}} + L\sqrt{\frac{m}{2eV}} \ . \quad (3.10)$$

In this relation L_0= 66 cm, L = 166 cm, T is the room temperature, k_B is the Boltzmann's constant = $1.380\text{X}10^{-23} JK^{-1}$, e is $1.67X10^{-19}$C. So, by the known value of the applied voltage in the ionization region, and the distance between the secondary ionization region to the accelerating region, one can find the time of flight of the particular fragment. From

equation 3.10 it is evident that the ions of different masses will arrive at the detector at different times. The arrival time is proportional to the square root of their mass.

3.6 Experimental Procedure

The pressure inside the chamber is maintained about 3X 10^{-7} Torr. A parallel beam of electrons from the primary electron gun is passed through the electrostatic lens system. This beam is further focused to the center of primary vacuum chamber by the lens system in the chamber. Focused beam interact with gas (CH_4) pulses exiting from the pulsing valve at the center of the primary chamber. After the interaction, different ionized and neutral fragments of CH_4 are produced and moved away from the interaction point. These, ionized fragments deflect from the deflector while the neutral fragments go straight to the secondary ionization region by travelling the distance L_0. In the secondary ionization region, these fragments are ionized by the threshold energy electrons from the filament. Thus formed positively ionized particles are repelled a distance d towards the ion accelerator by the positive voltage on ion repeller. When these ions enter into the ion accelerator they get accelerated and travel the distance L before reaching the MCP detector. The ion focusing lenses embedded in time of flight mass spectrometer help to focus them. The MCP detector detects the particles in different intervals of time that is mass dependent. On the basis of the detection time, one can distinguish the fragments. After the arrival of last fragment and making sure the vacuum in the primary chamber is normal, the second pulse of CH_4 is supplied. This process is continued until statistically significant fragment spectra are collected.

When the pulses of CH_4 molecules interact with the beam of electron at primary interaction region, some CH_4 may get fragmented while others might leave without fragmentation. Therefore, CH_4 along with the other neutral fragments reach the secondary ionization region. The spectra of the detected particles may contain the information about threshold ionized CH_4. In order to obtain only the TOF spectra resulting from neutrals created in the primary ionisation process, one should subtract threshold ionisation TOF spectra of CH_4 from the experimental TOF spectra. First, the experiment should be performed without applying primary electron beam and passing CH_4 gas pulses to threshold ionization region. Then the experiment is performed in the presence of primary electron beam. The differences between the peak intensities of the spectra of these two experiments can be used to obtain the production cross sections of neutral fragments.

3.7 Major Contribution by this Author to Ongoing Experimental Set-Up

The major contributions by this author are four fold: (1) building necessary vacuum systems, (2) building and testing lenses for primary electron beam, (3) estimation of probable neutral production cross sections, and (4) working on pulsing voltage power supply based on lab view program to operate the gas pulsing valve.

As shown in figure 3.1 major components in this experimental set-up are in a vacuum, that is bounded by one cylindrical chamber ($18^{"}$ I.D) and two tubes ($6^{"}$ I.D) connected in “cross” configuration with one end of the cross connecting to the cylindrical chamber. The cylindrical chamber and all other vacuum fittings are home built items. The whole system is placed 40 inches above the ground level supported by several vertical

poles and metal frames. The vacuum is created by three turbo- molecular pumps and their backing pumps. First, when the system was put in place and the pumps along with all the fitting were connected, there were several leaks in the low vacuum region (about 500 m Torr). These were corrected by smoothing surfaces and using appropriate vacuum sealers. There after the vacuum was reached about 12 mTorr with only backing pumps. This limit assures there aren't leaks in the rough vacuum regions because 12 mTorr is more or less the pumping limit for backing pumps. Next when the turbo pumps were turned –on and pumped for several days the pressure was dropped to 8x 10^{-6} Torr. As the original goal was to achieve low 10^{-7} Torr region and the pumps are capable in pumping to this level further leak tests were done by spraying acetone in to most likely leaking points. Upon finding those and sealing them the vacuum was dropped only down to 1x 10^{-6} Torr which is not adequate to run the experiment. After this point no leaks were detected by spraying acetone. Therefore the whole system was baked at about 110^0- 120^0C for about two weeks. Upon baking the vacuum was dropped to low 10^{-7} region. Last stage baking helped to get most of the oil and water out of the surfaces minimizing the out gassing rate.

The lens system that focuses the primary electron beam is a home built system. A sketch of this lens system is given in figure 3.5. It consists of three identical copper disks, each with $1^{"}$ diameter and $5/32^{"}$ thickness. Also, each disk is with a $3/16^{"}$ diameter center hole to pass electrons through. These disks are mounted in parallel configuration with a variable gap ($1/4$ - $1/8$ inch) between them. Plastic rods and spaces are used to keep the middle disk isolated from the two side ones and maintained a negative voltage in it while the two end disks are at ground potential.

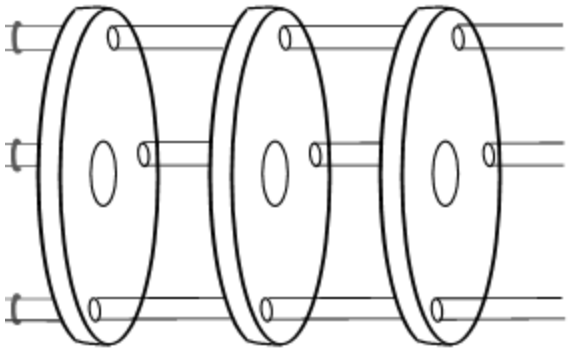

Fig. 3.5 The lens system used in the primary electron beam.

It is necessary to estimate the order of magnitude of the expected neutral production cross sections to decide the gas pulsing rate. This was accomplished by using experimental ion production cross section, elastic scattering cross section and total scattering cross section in equation 2.10. The estimated cross sections are in low $10^{-16} cm^2 to$ low $10^{-17} cm^2$ region as discussed in chapter two, section three. These ranges of the estimated cross sections are confirmed by independently using the existing theoretical cross sections in the literature in equation 2.10.

Lab view program is used to convert the output voltage of a 12 V DC power supply and this output voltage is used to operate the pulsing valve. A Pulse Width Modulation (PWM) signal of lab view is used in this conversion. A PWM signal consists of a duty cycle and a frequency. The duty cycle describes the amount of time for the signal to be in high state (on). The frequency determines how fast the PWM completes. Therefore, suitable values of frequencies can be used to set the DC power supply that enables the opening and closing mechanism of the pulsing valve.

CHAPTER FOUR

Conclusion

None of the groups yet experimentally measured the production cross section of all possible fragments of a particular molecule at the particular impact energy. There are three experiments found in the literature which measure some of the neutral fragments produced from methane (CH_4) by the impact of energetic electrons. But the results obtained are not in agreement to each other. Many theoretical approaches are also proposed for the estimation of the production cross sections of neutral fragments, but the results obtained by these approaches are also not in close agreement. In a comparison of experimental and theoretical work, it is evident that the production cross sections of neutral fragments obtained by them are not agreed to each other. The production cross sections of the neutral fragments are estimated to be 0.22-2.75X$10^{-16}cm^2$for the energy range 100 eV- 500 eV. An experimental arrangement, based on time of flight mass spectrometry, is designed for the better detection of neutral fragments. Currently, this experimental arrangement is in the process of building.

REFERENCES

1. Makochekanwa, C., Hoshino, M., Tanaka, H., & Kimura, M.(2007, October). Electron-Impact Induced Neutral Radical Fragmentation of CH_4. In Journal of Physics: Conference Series (vol. 86, No. 1, p. 012004). IOP Publishing.

2. Charles E. Melton and P.S. Rudolph. J. Chem., Phys. **47,** 1771 (1967).

3. **W**. Wang and N.D. Sze, Nature **286,** 589(1980).

4. F.G. Celii, P.E. Pehrsson, H. t. Wang and J.E. Butler, Appl. Lett. **52,** 2043 (1988).

5. Y. Hirose and Y. Terasawa, Jpn.J.Appl. Phys. **25,** L519 (1986).

6. M. Kimura, A. Igarashi, M. Imai, Y. Itikawa, M. Kitajima, T. Kusakabe, K. Moribyashi T. Morishita, K. Motohashi, L.Pichl, R. Suzuki, D.Kato, I.Murakami, T. Kato and M. Kato, NIFS-DATA-98 (2006).

7. N. Abramzon, K.E. Martus, and K. Becker., J. Chem. Phys. **113,** 2250 (2000).

8. Luna, H., M. Michael, M. B. Shah, R. E. Johnson, C. J. Latimer, and J. W. McConkey, Dissociation of N2 in capture and ionization collisions with fast H^+ and N^+ ions and modeling of positive ion formation in the Titan atmosphere, j. Geophysics. Res. 108 (0), 5033, doi: 10.1029/2002JE001950, 2003.

9. Tawara H and Phaneuf R A 1988 Comment. At. Mol. Phys. 11 177-93.

10. Total electron impact ionization cross sections for simple hydrocarbon molecules. Phys. B: At. Mol. Opt. Phys. 27 (1994) 2063.2074.

11. T.Nakano, H. Toyoda and H. Sugai, Jpn.J. Appl. Phys.**30,** 2908(1991), ibd. **30,** 2912 (1991).

12. S.Motlagh and J.H. Moore, J. Chem. Phys. **109,** 432(1998).

13. Daniel A. Erwin and Joseph A. Kunc, Phys. Rev. A **72**, 052719 (2005).

14. Daniel A. Erwin and Joseph A. Kunc, J.Appl. Phys **103,** 064906 (2008).

15. Christopher P. Goains , Ph.D. dissertation, Baylor University, Waco, TX (2004).

16. G. Garcia and F. Manero, J. Phys. B 29, 4017 (1996).

17. Electron- Molecule interactions and their applications by L.G. Chritophorou.

18. K.Gluch , P. Schier, W. Schustereder, T.Tepnual, L. Feketeova, C. Mair, S. Matt-Leubner, A. Stamatovic, T.D. Mark, Int. J. Mass Spectrum. **228** (2003) 307-320

19. S.Mondal, R. Shanker / Nucl. Instr. and Meth. in Phys. Res. B **246** (2006) 297-302.

20. Shyn T W J. Phys. B: At. Mol. Opt. Phys. **24** (1991) 5169-5173.

21. A. Zecca, G. Karwasz, R.S. Brusa, and C.Szmytkowski, J.Phys. B **24,** 2747(1991).

22. G. Garcia and F. Manero, Chem.Phys. Lett. **280,** 419 (1997).

23. G. Garcia and P. Manero, Phys. Rev. A **57,** 1069 (1998).

24. W.M. Ariyasinghe and D. Powers, Phys. Rev. A **66,** 052716 (2002).

25. Takeji Sakae, Shinchiro Sumiyoshi, Eiji Murakami, Yuzuru Matsumoto, Kenji Ishibashi and Akira Katase, J. Phys. B At. Mol. Phys. **22** (1989) 1385-1394.

26. Donald Rapp and Paula Englander Golden, j.Chem.Phys.**43, 1464** (1965).

27. H. Chatham, D. Hils, R. Robertson, and A. Gallagher j. Chem.Phys.**81**, 1770 (1984).

28. OJ Orient and SK Srivastava J. Phys. B: At. Mol. Phys. **20** (1987) 3923-3936.

29. H Nishimura and H Tawara, J. Phys. B: At. Mol. Opt. Phys. **27,** (1994) 2063-2074.

30. R.K. Janev and D. Reiter, "Collision Processes of Hydrocarbon Species in Hydrogen Plasmas; I. The Methane Family'', Report FZ- Julich Jul- 3966, Forchungszentrum Julich, Julich Germany (Feb.2002).

31. T. Shirai, T. Tabata, H. Tawara, and Y. Itikawa, At.Data Nucl. Data Tables **80**, 147 (2002).

32. www.kimphys.com/electron_guns/catalog_PDFs/Gun_intro_prelim.pdf.

BIBLIOGRAPHY

Abramzon N., Martus K.E., and Becker K., J. Chem. Phys. **113,** 2250 (2002)

Ariyasinghe W.M. and Powers D., Phys. Rev. A **66,** 052716 (2002).

Charles E. Melton and P.S. Rudolph. J. Chem., Phys. **47,** 1771 (1967).

Celii F.G., Pehrsson P.E., Wang H.t. and Butler J.E., Appl. Lett. **52,** 2043 (1988).

Chatham H., Hils H., Robertson R. and Gallagher A., j. Chem.Phys. **81**, 1770 (1984).

Christopher P. Goains , Ph.D. dissertation, Baylor University, Waco, TX (2004).

Daniel A. Erwin and Joseph A. Kunc, Phys. Rev. A **72,** 052719 (2005).

Daniel A. Erwin and Joseph A. Kunc, J.Appl. Phys **103,** 064906 (2008).

Donald Rapp and Paula Englander Golden, j.Chem.Phys.**43** ,1464 (1965).

Electron-Molecule interactions and their applications by L.G. Chritophorou..

Garcia G. and Manero F. J. Phys. B 29, 4017 (1996).

Garcia G. and Manero F. Chem.Phys. Lett. **280** ,419 (1997).

Garcia G. and Manero P. Phys. Rev. A **57,** 1069 (1998).

Gluch K. , Schier P.,Schustereder W., Tepnual T., Feketeova L., Mair C., Matt-Leubner S., Stamatovic A., Mark T.D., Int. J. Mass Spectrom. **228** (2003) 307-320.

Hirose Y. and Terasawa Y. Jpn.J.Appl. Phys. **25,** L519 (1986). Janev R.K. and Reiter D., "Collision Processes of Hydrocarbon Species in Hydrogen Plasmas: I. The Mehane Family" , Report FZ- Julich Jul-3966, Forchungszentrum Julich, Germany (Feb.2002).

Kimura M., Igarashi A., Imai M., Itikawa Y., Kitajima M., Kusakabe T., Moribayashi K., Morishita T., Motohashi K., Pichl L., Suzuki R., Kato D., Murakami I., Kato T., and Kato M.NIFS-DATA-98 (2006).

Luna, H., M. Michael, M. B. Shah, R. E. Johnson, C. J. Latimer, and J. W. McConkey, Dissociation of N2 in capture and ionization collisions with fast $H^+$and ions and modeling of positive ion formation in the Titan atmosphere, J. Geophysics. Res., 108 (0), 5033, doi:10.1029/2002JE001950, 2003.

Makochekanwa, C., Hoshino, M., Tanaka, H., & Kimura, M. (2007, October). Electron-Impact Induced Neutral Radical Fragmentation of CH_4 . In Journal of Physics: Conference Series (Vol.86, No.1, p.012004). IOP Publishing.

Motlagh S.and Moore J. H., J. Chem. Phys. **109,** 432(1998).

Mondal S., Shanker R. / Nucl. Instr. and Meth. in Phys. Res. B **246** (2006). 297-302.

Nakano T., Toyoda H. and Sugai H., Jpn.J. Appl. Phys.**30,** 2908(1991), ibd. **30,** 2912 (1991).

Nishimura H and Tawara H, J. Phys. B: At. Mol. Opt. Phys. **27,** (1994) 2063-2074.

Orient OJ and Srivastava SK J. Phys. B: At. Mol. Phys. **20** (1987) 3923-3936.

Parker Hannifin Corporation General Valve Division 19 Gloria Lane• Fairfield, NJ 07004.

Shirai T., Tabata T., Tawara H., and Itikawa Y. At.Data Nucl. Data Tables **80**,147 (2002).

Shyn T W J. Phys. B: At. Mol. Opt. Phys. **24** (1991) 5169-5173. Takeji Sakae, Shinchiro Sumiyoshi, Eiji Murakami, Yuzuru Matsumoto, Kenji Ishibashi and Akira Katase , J. Phys. B At. Mol. Phys.**22** (1989) 1385-1394.

Tawara H and Phaneuf R A 1988 Comment. At. Mol. Phys. 11 177-93.

Total electron impact ionization cross sections for simple hydrocarbon molecules. Phys. B: At. Mol. Opt.Phys. 27(1994)2063.2074.

Wang W. and Sze N. D., Nature **286,** 589(1980).

www.kimphys.com/electron_guns/catalog_PDFs/Gun_intro_prelim.pdf.

Zecca A., Karwasz G., Brusa R.S. and Szmytkowski C., J.Phys. B **24** , 2747(1991).